Published in final edited form as:
Exp Eye Res. 2013 June ; 111: 71–78. doi:10.1016/j.exer.2013.03.017.

RETINAL DEIMINATION AND PAD2 LEVELS IN RETINAS FROM DONORS WITH AGE-RELATED MACULAR DEGENERATION (AMD)

Vera L. Bonilha[a,*], **Karen G. Shadrach**[a], **Mary E. Rayborn**[a], **Yong Li**[a,b], **Gayle J. T. Pauer**[a], **Stephanie A. Hagstrom**[a], **Sanjoy K. Bhattacharya**[c], and **Joe G. Hollyfield**[a]

[a]Department of Ophthalmology, The Cole Eye Institute, Cleveland Clinic Lerner College of Medicine , Cleveland, OH, 44195, USA

[c]Bascom Palmer Eye Institute, University of Miami, Miami, FL, 33136, USA

Abstract

Deimination is a form of protein posttranslational modification carried out by the peptidyl arginine deiminases (PADs) enzymes. PAD2 is the principal deiminase expressed in the retina. Elevated levels of PAD2 and protein deimination are present in a number of human neurological diseases, with or without ocular manifestation. To define the association of deimination with the pathogenesis of age-related macular degeneration (AMD), we studied protein deimination and PAD2 levels in retinas of AMD donor eyes compared to age-matched non-AMD retinas. Eyes from non-AMD and AMD donors were fixed in 4% paraformaldehyde and 0.5% glutaraldehyde in phosphate buffer. Retina and retinal pigment epithelium (RPE) from donor eyes were processed for immunohistochemical detection and western blotting using antibodies to PAD2 and citrulline residues. The ganglion cell, inner plexiform, inner nuclear and outer nuclear layers were labeled by both PAD2 and citrulline antibodies. Changes in the localization of deiminated residues and PAD2 were evident as the retinal layers were remodeled coincident with photoreceptor degeneration in AMD retinas. Immunodetection of either PAD2 or citrulline residues could not be evaluated in the RPE layer due to the high autofluorescence levels in this layer. Interestingly, higher deimination immunoreactivity was detected in AMD retinal lysates. However, no significant changes in PAD2 were detected in the AMD and non-AMD retinas and RPE lysates. Our observations show increased levels of protein deimination but not PAD2 in AMD retinas and RPE, suggesting a reduced rate of turnover of deiminated proteins in these AMD retinas.

Keywords

Posttranslational modifications; protein deimination; immunohistochemistry; AMD; retina; retinal pigment epithelium

[*]Corresponding author: Vera L. Bonilha PhD, Cole Eye Institute (i31), Cleveland Clinic, 9500 Euclid Avenue, Cleveland OH 44195, Phone: 216-445-7690, Fax: 216-445-3670, bonilhav@ccf.org.
[b]Present affiliation: Department of Neurological Surgery, Case Western Reserve University, Cleveland, Ohio.

1. Introduction

Posttranslational modifications (PTMs) of proteins allow the incorporation of more structural and functional diversity in protein than is possible with only variations in amino acid residues. In turn PTMs become important as signals in the regulation of many cellular activities. Protein deimination, often referred to as citrullination, is a PTM that is carried out by peptidyl arginine deiminases (PADs) upon increase of intracellular calcium levels and involves conversion of arginine residues to citrulline (Vossenaar et al., 2003). Deimination of proteins induces a decrease in the charge of the modified proteins with major consequences on their conformation, stability and/or interactions with other proteins, and therefore on their functions (Gyorgy et al., 2006, Mechin et al., 2011). Mammalian cells possess five protein deiminases, PAD1-4 and 6 (Vossenaar et al., 2003).

PAD2 is considered the most prevalent isotype expressed in the central nervous system. Hence, elevated levels of PAD2 and protein deimination have been reported in a number of human neurological diseases including autoimmune encephalomyelitis (Nicholas et al., 2005), multiple sclerosis (Moscarello et al., 2007), Alzheimer's disease (Ishigami et al., 2005, Louw, et al., 2007; Mohlake and Whiteley, 2010; Acharya et al., 2012), Parkinson's disease (Nicholas, 2011), amyotrophic lateral sclerosis (Chou et al., 1996), and glaucoma (Bhattacharya et al., 2006a; Bhattacharya et al., 2006b; Cafaro et al., 2010). Elevated levels of PADs and protein deimination have also been linked to the pathogenesis of autoimmune diseases such as rheumatoid arthritis (Yamada et al., 2005, Harris et al., 2008, Kochi, 2010, Kochi et al., 2011, Giles et al., 2012).

Previously, it was reported that human brain from multiple sclerosis donors displayed increased deimination in comparison to brain from control and donors with other neurological diseases (Moscarello et al., 1994). The same study also found that infants possess higher levels of deimination compared to normal adults and that the relative proportion of relative deiminated protein in both multiple sclerosis and infant brain tissue was similar (Moscarello et al., 1994). We recently reported reduced levels of deimination in the retina, optic nerve, and blood of older F344BN rats compared to young animals. These observations were in concert with reduced mRNA and protein levels and activity for PAD2 in the retina and optic nerve of older rats compared to those from young rats (Bhattacharya et al., 2008). We also reported decreased deimination in ganglion cell layer together with increased deimination in other retinal layers to occur in a mouse model of demyelination (Pelizaeus-Merzbacher disease termed ND4 mice). These findings were accompanied by a decrease in inner retinal function indicating loss of vision in ND4 mice. In these mice, local restoration of deimination dramatically improved retinal function (Enriquez-Algeciras et al., 2013). Taken together, these findings suggest the cell-specific regulation of deimination may be a previously unrecognized indicator of retinal function. For example, increased deimination in astrocytes and decreased deimination in ganglion cells occurs in neurodegenerative disease. In contrast, increased deimination occurs in developing ganglion cells in infants. These results are consistent with our conjecture pertaining to differences in deimination in disease and development (Bhattachary, 2009).

Age-related macular degeneration (AMD) is the most common cause of irreversible blindness in the elderly population in industrialized countries. AMD is characterized by progressive loss of photoreceptors in the macula secondary to dysfunction of the retinal pigment epithelium (RPE) in the setting of prominent extracellular lesions. Late AMD can manifest in two forms, geographic atrophy or "dry AMD" and neovascular or "wet" AMD. Geographic atrophic (GA) is characterized by focal death of RPE, photoreceptors and choriocapillaris in the macula often together with large and abundant drusen accumulation (Biarnés et al., 2011). The 'wet'', neovascular form, occurs when new abnormal blood

vessels, originating from the choroid, penetrate Bruch's membrane causing damage to the RPE and overlying photoreceptors and resulting in vascular leakage, hemorrhage, and scarring (Freund et al., 2010). Dry AMD is much more common than wet, but choroidal neovascularization (CNV) in wet AMD accounts for the majority of vision loss (Bressler et al., 1988). The purpose of this study was to define the distribution of protein deimination and PAD2 in eyes from donors with AMD and to compare this with the distribution in age-matched non-AMD eyes. We found that the amount of protein deimination but not the levels of PAD2 was significantly increased in retinal and RPE lysates from AMD donor eyes, as compared to that observed from non-AMD eyes. All together our data suggests that strict, localized regulation of deimination levels is essential for retinal function.

2. Material and methods

2.1. Human eye tissue

Donor eyes were obtained from the Cleveland Eye Bank or through the Foundation Fighting Blindness Eye (FFB) Donor Program (Columbia, MD). Tissue from 41 different donors was analyzed. Among those, 16 samples were from non-AMD donors and 25 were from AMD donors. The analyzed tissue included FFB donations # 703, 704, 711, 714, 716, 722, 723, 728, 745, 758, 781. The donor ages varied between 35 and 91 years and the interval between time of death and tissue processing varied between 4 and 35.5 hours. Additional information about the donors is provided in table 1. Eye bank records accompanying the donor eyes indicated whether the donor had AMD or no known eye diseases. One eye from each donor was used in our analysis. Globes were cut trough the *ora serrata* and individually assessed for gross pathology using a Zeiss Universal S3 surgical microsocope with an OPMI MD Microscopic Head equipped with a Xenon Light Source. Upon dissection, the fundus of each eye was analyzed, and graded according to the AREDS disease stage using the Minnesota grading system for post-mortem eyes as defined by the location and area of drusen distribution (Olsen and Feng, 2004). In our samples we could not determine if subretinal drusenoid deposits were present. Fixed eyes were analyzed intact, with the retina on top of the RPE, while unfixed tissue had the retina mechanically removed from the RPE before grading the eyes. Of the AMD eyes used in this analysis, 7 had advanced AMD, defined as either neovascular AMD or geographic atrophy (GA) involving the center of the macula, and the remaining eyes were either stage 2 or 3. Non-AMD control eyes did not have any drusen in the macular area nor did they display any grossly visible AMD features. The immunohistochemical and western blot analysis of these eyes is exempt of IRB approval.

Macroscopic fundus images were collected using a Zeiss AxioCam MRC5 camera equipped with a macro video lens. Prior to imaging, the cornea and lens were removed leaving only the posterior pole. Remaining eyecups were filled with PBS to eliminate specular reflections and improve contrast and image quality.

2.2. Preparation of human RPE and retina lysates

RPE cells (Table 1) were isolated using the protocol initially described with mechanical removal of the retina and brushing of the RPE from the choroid in PBS (Nakata et al., 2005). RPE cells suspended in PBS were pelleted, the PBS was aspirated from the tube and fresh PBS containing protease inhibitors was added to the cells. The RPE cells were kept at −80°C until used. RPE lysates were diluted 1:1 with 2X radioimmunoprecipitation buffer (RIPA) (0.2% SDS, 2% Triton X 100, 2% deoxycholate, 0.15M NaCl, 4mM EDTA, 50mM Tris pH 7.4) containing a cocktail of protease and phosphatase inhibitors (Sigma, St. Louis, MO, USA). Pieces of retinas collected from human donor eyes were collected into eppendorff tubes and lysed in 1X RIPA buffer. Cells were lyzed for 1 h at 4°C in a rotator, centrifuged for 10 min at 14000rpm and the supernatants were transferred to clean tubes. The protein

concentration was determined using the MicroBCA kit (Pierce Biotechnology, Inc., Rockford, IL) according to the manufacture's directions.

2.3 Western blot analysis of lysates

Protein from each sample (40μg) was boiled in SDS sample buffer (62.5 mMTris-HCl (pH 6.8), 25% glycerol, 0.01% bromophenol blue, and 2% SDS), separated on a 10–20% Novex®-Tris-Glycine gel (Invitrogen Corporation, Carlsbad, CA) and electro-transferred to Immobilon PVDF membranes (Millipore, Bedford, MA) using a Bio-Rad Semi-Dry Electrophoretic Transfer Cell (20 min transfer at 18 volts). Membranes were incubated with antibodies to modified citrulline (#17–347, from the Anti-Citrulline (modified) Detection Kit, EMD Millipore, Lake Placid, NY) and PAD2 (ab16478, Abcam, Cambridge, MA) in Blotto A buffer (20 mM Tris/HCl, 0.9% NaCl, 0.05% Tween 20 (TBST), 5% skimmed milk) for 1h. For detection of deimination, PVDF membranes were incubated at 37°C overnight without agitation with modification buffer, prepared by mixing 1 part of reagent A (0.025% $FeCl_3$ in a solution of sterile, distilled water/98%H_2SO_4/ 85%H_3PO_4 (55%/25%/ 20%)) and 1 part of reagent B (0.5% 2,3-butanedione monoxime, 0.25% antipyrine, 0.5M acetic acid) as described in the anti-citrulline (modified) detection kit (Millipore). After extensive washing and blocking, membranes were reacted with secondary antibodies conjugated to peroxidase and signal was visualized using chemiluminescence Reagent Plus (NEN™ Life Science Products, Inc., Boston, MA) detection system.

The gels were stained with Gelcode Blue (Thermo Scientific, Rockford, IL), after partial transfer to PVDF membranes to serve as a reference for the load homogeneity of the samples as previously described (Bando et al., 2007; Bonilha et al., 2008). Briefly, both gel and blot were digitized using a densitometer (BIO-RAD GS800), and the density of the gel and bands was measured and transferred to pixels using Quantity One 4.6.8. A rectangular area was drawn around the most intense band signal in the scanned blots and used as a template to determine the number of pixels in these areas. Plotted signals represent pixel intensity for each band after subtraction from the background signal. The total protein pixel number from each donor lane stained with Gelcode Blue in the transferred gel was quantified. The previously determined number of pixels in the Western blot was divided by the pixels in the Gelcode Blue lane, and these then were used to establish the pixel count per sample. The average pixel count was determined as a mean of all the AMD and non-AMD samples. Standard error and t-test were calculated using GraphPad Softaware (http://www.graphpad.com/quickcalcs/ttest1.cfm) and are presented in Section 3.

2.4. Immunohistology of tissue

The presence of deiminated proteins was investigated in cryosections of AMD and non-AMD eyes in the perifoveal area (between the fovea and the optic nerve head). Eye pieces of retina-RPE-choroid were cut and fixed by immersion in 4% paraformaldehyde made in PBS overnight at 4°C, quenched with 50mM NH_4Cl made in PBS for 1h at 4°C, infused successively with 10% and 20% sucrose made in the same buffer and with Tissue-Tek "4583" (Miles Inc., Elkhart, IN). 10–12μm cryosections were cut on a cryostat HM 505E (Microm, Walldorf, Germany) equipped with a CryoJane Tape-Transfer system (Instrumedics, Inc., Hackensack, NJ, USA). For detection of protein deimination, cryosections of retina-RPE-choroid were processed and labeled using anti-citrulline (modified) detection kit as described in western blot analysis. Briefly, cryosections of retina-RPE-choroid were hydrated, the freezing medium (3 parts of 20% sucrose made in PBS to 7 parts of Tissue-Tek "4583") was removed and cryosections of retina-RPE-choroid were treated with freshly made modification buffer for 30 min. at 37°C. Tissue was blocked in PBS supplemented with + 1% BSA (PBS/BSA) for 30 min, and incubated with the antibodies to protein deimination (Millipore) and PAD2. The monoclonal PAD2 antibody

has been previously described and characterized in rat retinas (Koike et al., 1994; Bhattacharya et al., 2008). Cell nuclei were labeled with TO-PRO®-3 iodide (Molecular Probes). Secondary antibody (goat anti-rabbit IgG; 1:1000) was labeled with Alexa Fluor 488. Sections were analyzed using a Leica laser scanning confocal microscope (TCS-SP2, Leica, Exton, PA). A series of 1μm *xy* (*en face*) sections were collected. Each individual *xy* image of the retinas stained represents a three-dimensional projection of the entire cryosection (sum of all images in the stack). Microscopic panels were composed using Adobe Photoshop CS3 (Adobe, San Jose, CA). The labeling controls were incubated with secondary antibodies only.

2.5. Genetic Analysis of AMD samples

Several of the donor samples (11 non-AMD and 25 AMD) were genotyped for single nucleotide polymorphisms (SNPs) previously shown to be associated with the development and progression of AMD. DNA was extracted from blood or eye tissue by means of the Gentra Systems PUREGENE DNA Purification kit (Qiagen, Minneapolis, MN). Samples were genotyped for SNPs rs1061170 (*CFH*), rs10490924 (*ARMS2*), rs11200638 (*HTRA1*), and rs2230199 (*C3*), using TaqMan SNP genotyping assays.

3. Results

3.1. Immunolocalization of deimination in retinas of AMD donors

To define the localization of deiminated proteins and PAD2 in the retina of AMD donors several samples were analyzed. Representative fundus images are presented in Fig. 1 of one non-AMD eye (Fig.1A) and four advanced AMD eyes (Fig.1B to 1E). Evidence for GA (Fig. 1B and 1C) and neovascular AMD (Fig. 1D and 1E) can be observed in the areas selected for histological analysis (Fig. 1, rectangles).

The distribution of deiminated proteins from perimacular areas of non-AMD (Fig. 2A, 2D) and in AMD retinas (Fig. 2B, 2C, 2E, 2F) is illustrated in Fig. 2. Analysis of the retinal sections showed that the localization of immunoreactivity of deiminated proteins in AMD retinas was similar to that observed in non-AMD retinas. Specifically, labeling was observed in ganglion cell, inner nuclear layer and outer nuclear layer as well as the choroid in non-AMD retinas (Fig.2A) when deimination labeling was overlaid on differential contrast images (DIC) of the retina. Interestingly, deimination immunoreactivity was mostly localized to the nuclei of cells in each of these locations. A disorganized distribution of deiminated proteins was evident in the degenerated areas of the retinas of AMD donors due to retina modeling as evidenced by the retina morphology (Fig. 2B, 2C, 2E, 2F, braces). Non-AMD (Fig. 2D) and AMD (data not shown) retinas labeled only with the secondary antibody did not display any deiminated protein labeling.

3.2. Similar immunolocalization of PAD2 in retinas of several AMD donors

The distribution of PAD2 was also analyzed in the perimacula of AMD and non-AMD retinas (Fig. 3). Interestingly, PAD2 immunoreactivity was stronger and more abundant than deimination. PAD2 was detected in all retinal lamina in both non-AMD (Fig. 3A) and AMD retinas from several donors (Fig.3B, 3C, 3E, 3F). PAD2 also localized to the nuclei of cells in the ganglion cell layer, and the inner and outer nuclear layer. A disorganized distribution of PAD2 was evident in the degenerated areas of the retinas of AMD donors (Fig. 3B, 3C, 3E, 3F, braces). Non-AMD (Fig. 3D) and AMD (data not shown) retinas labeled only with the secondary antibody did not display any PAD2 labeling; non- AMD retina displayed typical laminar organization.

3.3. Protein deimination in RPE and retina lysates of AMD donors

The intensity of immunoreactivity of deiminated protein within the AMD and non-AMD RPE and retinas were separately analyzed by western blot analysis using anti-modified citrulline antibody and comparison to gels stained with Gelcode blue after partial transfer to PVDF membranes to serve as reference for the load homogeneity of the samples (Fig.4A and 4D). Our analysis revealed significant increase in the immunoreactivity in AMD RPE lysates (Fig.4B, lane 5 to 8) when compared to non-AMD retinas (Fig.4B, lane 1 to 4). The specificity of the immunoreactivity was demonstrated by reacting Drosophila (canton S strain) whole extract, which lacks PADs (Fig.4B, lane 9), and Drosophila whole extract that has been subjected to citrullination with PAD2 incubation (Fig.4B, lane 10). Significant increase in the deiminated immunoreactivity was also observed in AMD (Fig.4E, lane 5 to 8) and non-AMD retinal lysates (Fig.4E, lane 1 to 4). The deiminated proteins in RPE lysates showed several prominent protein bands (ca. between 82 and 49 kDa and ~200kDa, Fig.4B). In contrast, the retinal lysates displayed several major bands in the molecular weight range 37–64 kDa (Fig.4E). Immunoblot quantification of RPE and retina lysates obtained from AMD donor eyes displayed significant increase in protein deimination immunoreactivity intensity (Fig.4C and 4F). Quantitation of these blots showed that protein deimination immunoreactivity was upregulated 1.8 fold in AMD RPE and 2.2 fold in AMD retina samples when compared with non-AMD samples. These differences were statistically significant ($p=0.0164$ in the RPE and $p=0.0481$ in the retinas) (Fig.4C and 4F).

3.4. PAD2 in RPE and retina lysates of AMD donors

The differences in immunoreactivity of PAD2 within the AMD and non-AMD RPE and retinas were addressed by Western analysis. Whole RPE (Fig.5A to 5C) and retina (Fig.5D to 5F) lysates were harvested, resolved in a SDS-PAGE and transferred to a membrane and reacted with PAD2 antibody. Western blot using anti-PAD2 antibody revealed no significant differences in the immunoreactivity between non-AMD (Fig.5B, lane 1 to 4) and AMD (Fig. 5B, lane 5 to 8) RPE lysates. Similar observations were also made for non-AMD (Fig.5E, lane 1 to 4) and AMD retinal (Fig.5E, lane 5 to 8) lysates probed with anti-PAD2 antibody. Quantitation of these blots showed PAD2 immunoreactivity was upregulated 1.2 fold in both AMD RPE and retina samples when compared with non-AMD samples. However, these differences were not statistically significant ($p=0.2193$ in RPE and $p=0.4535$ in retinas) (Fig. 5C and 5F).

3.5. No differential genetic association in AMD compared to non-AMD donors

Among the donor tissue studied, 11 non-AMD and 25 AMD were genotyped for four SNPs previously associated with the risk and progression of AMD. These included: 1) complement factor H (*CFH*) Y402H (rs1061170), (2) age-related maculopathy susceptibility 2 (*ARMS2*, also called LOC387715) A69S (rs10490924), (3) high temperature requirement factor A1 (*HTRA1*) (rs11200638), and (4) complement component 3 (*C3*) R80G (rs2230199). The minor allele frequencies for each SNP are shown in Table 2. There was no significant difference between the AMD samples and the non-AMD samples at any of the SNPs.

4. Discussion

Deimination is a form of protein PTM involving conversion of arginine residues into citrulline. This reaction is carried out by PAD2 in the retina. Previously, we observed lower levels on proteins deimination in the retina and optic nerve as well as reduced blood levels in older rats compared to young animals. The purpose of this investigation was to define the distribution and relative levels of protein deimination and PAD2 in retinal tissues from AMD donor eyes for comparison with these tissues from age-matched non-AMD eyes. We

found that deiminated proteins were highest in AMD tissues, but PAD2 levels were not increased above those present in non-AMD tissues. To our knowledge this is the first report on citrullination in retinas of donors with AMD.

The calcium-dependent enzymatic deimination of peptidyl- arginine to peptidyl-citrulline, leads to a decrease in the charge of the modified proteins with major consequences on their conformation, stability and/or interactions. In turn, this affects their functions (Mechin et al., 2011). The physiologic significance of deimination is yet to be defined.

It has been reported that PAD2 activity in damaged neuronal tissue is often triggered by calcium imbalance (Asaga and Ishigami, 2001; Asaga et al., 2002). We did not specifically measure Ca^{2+} levels in the samples analyzed. However, several reports suggest that changes in Ca^{2+}-signaling are observed in AMD retinas and may be a factor modulating PAD2 activity in AMD retinas (Spraul and Grossniklaus, 1997; Li et al., 2010; Vogt et al., 2011; Chen et al., 2012). First, oxidative stress, an important cause of retinal pigment epithelium death and subsequent AMD, induces calcium overload and leads to cell injury (Li et al., 2010). Second, it has been shown that all-trans-retinal-mediated photoreceptor degeneration *in vivo* is associated with changes in $PLC/IP_3/Ca^{2+}$ signaling (Chen et al., 2012). Third, calcification of Bruch's membrane has been reported in postmortem eyes from AMD donors (Spraul and Grossniklaus, 1997) and is increased in geographic atrophy eyes (Vogt et al., 2011). Fourth, calcification is an end-stage of drusen (Rudolf et al., 2008).

Variability was observed in the PAD2 immunoreactivity and protein deimination in the AMD and non-AMD retinal lysates. This observation may be related to different genetic markers and environmental factors associated with each sample. Indeed, it is known that genetic factors and environment influence susceptibility to AMD (Smith et al., 2001; Chen et al., 2010; Chen et al., 2011; Choudhury et al., 2011; Seddon et al., 2011). However, our analysis of the four SNPs that are consistently shown to have the strongest associations with the development and progression of AMD revealed no difference between AMD and non-AMD samples. These results suggest that genetic risk factors do not influence deimination of proteins in AMD retinas. Environmental factors such as smoking have been linked to deimination in both rheumatoid arthritis and multiple sclerosis (Klareskog et al., 2006a, Klareskog et al., 2006b; Mahdi et al., 2009; Kochi et al., 2011). However, the information available for the tissue analyzed did not include donors smoking habits.

Our unpublished data determined that the levels of PAD1, PAD3 and PAD4 remains unchanged in the AMD tissue compared to controls using quantitative amplified message (real time PCR). In addition, almost none or very low levels of PAD1 and PAD3 protein were detected in RPE lysates. Therefore, the changes in citrullination reported here are likely related to PAD2 activity.

In conclusion, we found that protein deimination but not PAD2 was significantly increased in AMD retinas and RPE lysates. While PAD2 levels were not significantly increased in AMD tissue, it is possible that its enzymatic activity is different in AMD samples, while the level of PAD2 remains the same. It is also possible that in AMD samples, the deiminated proteins accumulate due to reduced turnover/lysosomal and/or proteasomal function. Indeed, RPE lysosomal activity is a cellular function reported to be altered in AMD (Beatty et al., 2000; Mettu et a, 2012). In addition, increased expression of proteins involved in the proteasomal pathway was also reported in the retinas of AMD donors (Ethen et al., 2006, Ethen et al., 2007).

Our results, suggest that protein deimination may have a role in the pathology of AMD and that deiminated proteins might become a useful biomarker for neurodegeneration in this disease. Our experiments did not address the identity of proteins deiminated in the AMD

retinas. Previously, immunoprecipitation and mass spectrometry have identified about 36 proteins that potentially undergo deimination in the human retina (Bhattacharya, 2009). Several of these proteins could be citrullinated in AMD retinas leading to changes in their biological activity. Alternatively, it is possible that molecules involved in soft tissue calcification such as pyrophosphate, fetuin A, matrix gla protein, vitamin K, and ATP-binding cassettes 6, among other proteins may be regulated through deimination in the retina.

Acknowledgments

Supported by NIH grants EY014240 (JGH), a Research Center Grant from the Foundation Fighting Blindness (JGH), a Challenge Grant from Research to Prevent Blindness (JGH) and Research to Prevent Blindness career award (SKB).

References

Acharya NK, Nagele EP, Han M, Coretti NJ, DeMarshall C, Kosciuk MC, Boulos PA, Nagele RG. Neuronal PAD4 expression and protein citrullination: possible role in production of autoantibodies associated with neurodegenerative disease. J. Autoimmun. 2012; 38:369–380. [PubMed: 22560840]

Asaga H, Ishigami A. Protein deimination in the rat brain after kainate administration: citrulline-containing proteins as a novel marker of neurodegeneration. Neurosci. Lett. 2001; 299:5–8. [PubMed: 11166924]

Asaga H, Akiyama K, Ohsawa T, Ishigami A. Increased and type II-specific expression of peptidylarginine deiminase in activated microglia but not hyperplastic astrocytes following kainic acid-evoked neurodegeneration in the rat brain. Neurosci. Lett. 2002; 326:129–132. [PubMed: 12057845]

Beatty S, Koh H, Phil M, Henson D, Boulton M. The role of oxidative stress in the pathogenesis of age-related macular degeneration. Surv Ophthalmol. 2000; 45:115–134. [PubMed: 11033038]

Bando H, Shadrach KG, Rayborn ME, Crabb JW, Hollyfield JG. Clathrin and adaptin accumulation in drusen, Bruch's membrane and choroid in AMD and non-AMD donor eyes. Exp. Eye Res. 2007; 84:135–142. [PubMed: 17097084]

Bhattacharya SK, Bhat MB, Takahara H. Modulation of peptidyl arginine deiminase 2 and implication for neurodegeneration. Curr. Eye Res. 2006a; 31:1063–1071. [PubMed: 17169845]

Bhattacharya SK, Crabb JS, Bonilha VL, Gu X, Takahara H, Crabb JW. Proteomics implicates peptidyl arginine deiminase 2 and optic nerve citrullination in glaucoma pathogenesis. Invest. Ophthalmol. Vis. Sci. 2006b; 47:2508–2514. [PubMed: 16723463]

Bhattacharya SK, Sinicrope B, Rayborn ME, Hollyfield JG, Bonilha VL. Age-related reduction in retinal deimination levels in the F344BN rat. Aging Cell. 2008; 7:441–444. [PubMed: 18248664]

Bhattacharya SK. Retinal deimination in aging and disease. IUBMB Life. 2009; 61:504–509. [PubMed: 19391158]

Biarnés M, Monés J, Alonso J, Arias L. Update on Geographic Atrophy in Age-Related Macular Degeneration. Optom Vis Sci. 2011; 88:881–889. [PubMed: 21532519]

Bonilha VL, Rayborn ME, Shadrach KG, Li Y, Lundwall A, Malm J, Hollyfield JG. Semenogelins in the human retina: Differences in distribution and content between AMD and normal donor tissues. Exp. Eye Res. 2008; 86:150–156. [PubMed: 18036592]

Bressler NM, Frost LA, Bressler SB, Murphy RP, Fine SL. Natural course of poorly defined choroidal neovascularization associated with macular degeneration. Arch Ophthalmol. 1988; 106:1537–1542. [PubMed: 2461191]

Cafaro TA, Santo S, Robles LA, Crim N, Urrets-Zavalia JA, Serra HM. Peptidylarginine deiminase type 2 is over expressed in the glaucomatous optic nerve. Mol. Vis. 2010; 16:1654–1658. [PubMed: 20806090]

Chen Y, Bedell M, Zhang K. Age-related macular degeneration: genetic and environmental factors of disease. Mol. Interv. 2010; 10:271–281. [PubMed: 21045241]

Chen Y, Okano K, Maeda T, Chauhan V, Golczak M, Maeda A, Palczewski K. Mechanism of all-trans-retinal toxicity with implications for stargardt disease and age-related macular degeneration. J. Biol. Chem. 2012; 287:5059–5069. [PubMed: 22184108]

Chen Y, Zeng J, Zhao C, Wang K, Trood E, Buehler J, Weed M, Kasuga D, Bernstein PS, Hughes G, Fu V, Chin J, Lee C, Crocker M, Bedell M, Salasar F, Yang Z, Goldbaum M, Ferreyra H, Freeman WR, Kozak I, Zhang K. Assessing susceptibility to age-related macular degeneration with genetic markers and environmental factors. Arch. Ophthalmol. 2011; 129:344–351. [PubMed: 21402993]

Chou SM, Wang HS, Taniguchi A. Role of SOD-1 and nitric oxide/cyclic GMP cascade on neurofilament aggregation in ALS/MND. J. Neurol. Sci. 1996; 139(Suppl):16–26. [PubMed: 8899653]

Choudhury F, Varma R, McKean-Cowdin R, Klein R, Azen SP. Risk factors for four-year incidence and progression of age-related macular degeneration: the los angeles latino eye study. Am. J. Ophthalmol. 2011; 152:385–395. [PubMed: 21679916]

Enrique-Algeciras M, Ding D, Mastronardi FG, Marc RE, Porciatti V, Bhattacharya SK. Deimination restores inner retinal visual function in a demyelinating disease. J. Clin. Inv. 2013 in press.

Ethen CM, Reilly C, Feng X, Olsen TW, Ferrington DA. The proteome of central and peripheral retina with progression of age-related macular degeneration. Invest Ophthalmol Vis Sci. 2006; 47:2280–2290. [PubMed: 16723435]

Ethen CM, Hussong SA, Reilly C, Feng X, Olsen TW, Ferrington DA. Transformation of the proteasome with age-related macular degeneration. FEBS Lett. 2007; 581:885–890. [PubMed: 17289037]

Freund KB, Zweifel SA, Engelbert M. Do we need a new classification for choroidal neovascularization in age-related macular degeneration? Retina. 2010; 30:1333–1349. [PubMed: 20924258]

Giles JT, Fert-Bober J, Park JK, Bingham CO 3rd, Andrade F, Fox-Talbot K, Pappas D, Rosen A, van Eyk J, Bathon JM, Halushka MK. Myocardial citrullination in rheumatoid arthritis: a correlative histopathologic study. Arthritis Res Ther. 2012; 14:R39. [PubMed: 22364592]

Gyorgy B, Toth E, Tarcsa E, Falus A, Buzas EI. Citrullination: a posttranslational modification in health and disease. Int. J. Biochem. Cell Biol. 2006; 38:1662–1677. [PubMed: 16730216]

Harris ML, Darrah E, Lam GK, Bartlett SJ, Giles JT, Grant AV, Gao P, Scott WW Jr. El-Gabalawy H, Casciola-Rosen L, Barnes KC, Bathon JM, Rosen A. Association of autoimmunity to peptidyl arginine deiminase type 4 with genotype and disease severity in rheumatoid arthritis. Arthritis Rheum. 2008; 58:1958–1967. [PubMed: 18576335]

Ishigami A, Ohsawa T, Hiratsuka M, Taguchi H, Kobayashi S, Saito Y, Murayama S, Asaga H, Toda T, Kimura N, Maruyama N. Abnormal accumulation of citrullinated proteins catalyzed by peptidylarginine deiminase in hippocampal extracts from patients with Alzheimer's disease. J. Neurosci. Res. 2005; 80:120–128. [PubMed: 15704193]

Klareskog L, Padyukov L, Lorentzen J, Alfredsson L. Mechanisms of disease: Genetic susceptibility and environmental triggers in the development of rheumatoid arthritis. Nat. Clin. Pract. Rheumatol. 2006a; 2:425–433. [PubMed: 16932734]

Klareskog L, Stolt P, Lundberg K, Kallberg H, Bengtsson C, Grunewald J, Ronnelid J, Harris HE, Ulfgren AK, Rantapaa-Dahlqvist S, Eklund A, Padyukov L, Alfredsson L. A new model for an etiology of rheumatoid arthritis: smoking may trigger HLA-DR (shared epitope)-restricted immune reactions to autoantigens modified by citrullination. Arthritis Rheum. 2006b; 54:38–46. [PubMed: 16385494]

Kochi Y. Genetic background of tolerance breakdown in rheumatoid arthritis. Nihon Rinsho Meneki Gakkai Kaishi. 2010; 33:48–56. [PubMed: 20453439]

Kochi Y, Thabet MM, Suzuki A, Okada Y, Daha NA, Toes RE, Huizinga TW, Myouzen K, Kubo M, Yamada R, Nakamura Y, Yamamoto K. PADI4 polymorphism predisposes male smokers to rheumatoid arthritis. Ann. Rheum. Dis. 2011; 70:512–515. [PubMed: 21062850]

Koike H, Sase K, Uchida H, Sudo T, Shiraiwa M, Sugawara K, Takahara H. Production and epitope specificity of monoclonal antibody against mouse peptidylarginine deiminase type II. Biosci. Biotechnol. Biochem. 1994; 58:2286–2287. [PubMed: 7530067]

Li GY, Fan B, Zheng YC. Calcium overload is a critical step in programmed necrosis of ARPE-19 cells induced by high-concentration H(2)O(2). Biomed. Environ. Sci. 2010; 23:371–377. [PubMed: 21112485]

Louw C, Gordon A, Johnston N, Mollatt C, Bradley G, Whiteley CG. Arginine deiminases: therapeutic tools in the etiology and pathogenesis of Alzheimer's disease. J. Enzyme Inhib. Med. Chem. 2007; 22:121–126. [PubMed: 17373558]

Mahdi H, Fisher BA, Kallberg H, Plant D, Malmstrom V, Ronnelid J, Charles P, Ding B, Alfredsson L, Padyukov L, Symmons DP, Venables PJ, Klareskog L, Lundberg K. Specific interaction between genotype, smoking and autoimmunity to citrullinated alpha-enolase in the etiology of rheumatoid arthritis. Nat. Genet. 2009; 41:1319–1324. [PubMed: 19898480]

Mechin MC, Nachat R, Coudane F, Adoue V, Arnaud J, Serre G, Simon M. Deimination or citrullination, a post-translational modification with many physiological and pathophysiological facets. Med. Sci. (Paris). 2011; 27:49–54. [PubMed: 21299962]

Mettu PS, Wielgus AR, Ong SS, Cousins SW. Retinal pigment epithelium response to oxidant injury in the pathogenesis of early age-related macular degeneration. Mol. Aspects Med. 2012; 33:376–398. [PubMed: 22575354]

Mohlake P, Whiteley CG. Arginine metabolising enzymes as therapeutic tools for Alzheimer's disease: peptidyl arginine deiminase catalyses fibrillogenesis of beta-amyloid peptides. Mol. Neurobiol. 2010; 41:149–158. [PubMed: 20224908]

Moscarello MA, Wood DD, Ackerley C, Boulias C. Myelin in multiple sclerosis is developmentally immature. J Clin Invest. 1994; 94:146–154. [PubMed: 7518827]

Moscarello MA, Mastronardi FG, Wood DD. The role of citrullinated proteins suggests a novel mechanism in the pathogenesis of multiple sclerosis. Neurochem. Res. 2007; 32:251–256. [PubMed: 17031564]

Nakata K, Crabb JW, Hollyfield JG. Crystallin distribution in Bruch's membrane-choroid complex from AMD and age-matched donor eyes. Exp. Eye Res. 2005; 80:821–826. [PubMed: 15939038]

Nicholas AP. Dual immunofluorescence study of citrullinated proteins in Parkinson diseased substantia nigra. Neurosci. Lett. 2011; 495:26–29. [PubMed: 21414385]

Nicholas AP, Sambandam T, Echols JD, Barnum SR. Expression of citrullinated proteins in murine experimental autoimmune encephalomyelitis. J. Comp. Neurol. 2005; 486:254–266. [PubMed: 15844173]

Olsen TW, Feng X. The Minnesota Grading System of eye bank eyes for age-related macular degeneration. Invest. Ophthalmol. Vis. Sci. 2004; 45:4484–4490. [PubMed: 15557458]

Rudolf M, Clark ME, Chimento MF, Li CM, Medeiros NE, Curcio CA. Prevalence and Morphology of Druse Types in the Macula and Periphery of Eyes with Age-Related Maculopathy. Invest. Ophthalmol. Vis. Sci. 2008; 49:1200–1209. [PubMed: 18326750]

Seddon JM, Reynolds R, Yu Y, Daly MJ, Rosner B. Risk models for progression to advanced age-related macular degeneration using demographic, environmental, genetic, and ocular factors. Ophthalmology. 2011; 118:2203–2211. [PubMed: 21959373]

Smith W, Assink J, Klein R, Mitchell P, Klaver CC, Klein BE, Hofman A, Jensen S, Wang JJ, de Jong PT. Risk factors for age-related macular degeneration: Pooled findings from three continents. Ophthalmology. 2001; 108:697–704. [PubMed: 11297486]

Spraul CW, Grossniklaus HE. Characteristics of Drusen and Bruch's membrane in postmortem eyes with age-related macular degeneration. Arch. Ophthalmol. 1997; 115:267–273. [PubMed: 9046265]

Vogt SD, Curcio CA, Wang L, Li CM, McGwin G Jr. Medeiros NE, Philp NJ, Kimble JA, Read RW. Retinal pigment epithelial expression of complement regulator CD46 is altered early in the course of geographic atrophy. Exp. Eye Res. 2011; 93:413–423. [PubMed: 21684273]

Vossenaar ER, Zendman AJ, van Venrooij WJ, Pruijn GJ. PAD, a growing family of citrullinating enzymes: genes, features and involvement in disease. Bioessays. 2003; 25:1106–1118. [PubMed: 14579251]

Yamada R, Suzuki A, Chang X, Yamamoto K. Citrullinated proteins in rheumatoid arthritis. Front Biosci. 2005; 10:54–64. [PubMed: 15574347]

- PAD2 and citrulline retina.
- PAD2 relocalized in AMD.
- Increased citrulline in AMD.

- PAD2 and citrulline antibodies labeled the ganglion cell, inner plexiform, inner nuclear and outer nuclear layers.
- Changes in the localization of deiminated residues and PAD2 were evident as the retinal layers were remodeled coincident with photoreceptor degeneration in AMD retinas.
- Higher deimination immunoreactivity of protein deimination but not PAD2 in AMD retinas and RPE lysates were detected.

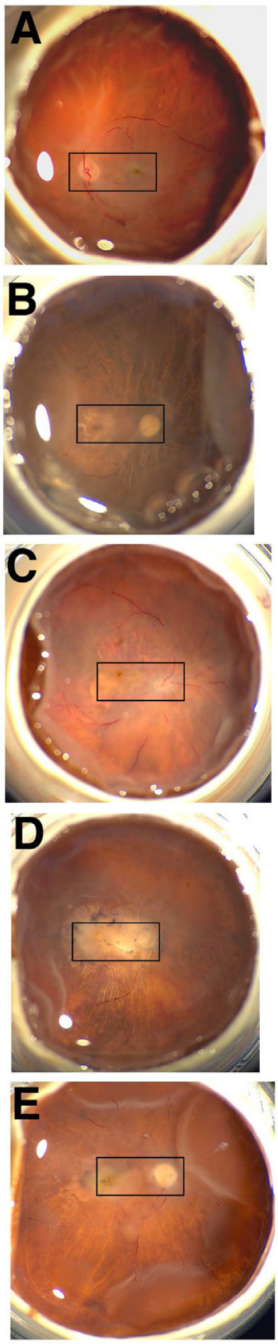

Fig. 1. *In situ* imaging of whole AMD and age-matched non-AMD donor eyes

The optic nerve head, macula and retinal veins were visible in the macroscopic fundus image of the non-AMD eye (A). AMD samples displayed typical geographic atrophy (B, D) and exudate accumulation around the macula (C–E). Rectangles highlight the areas selected for histological analysis.

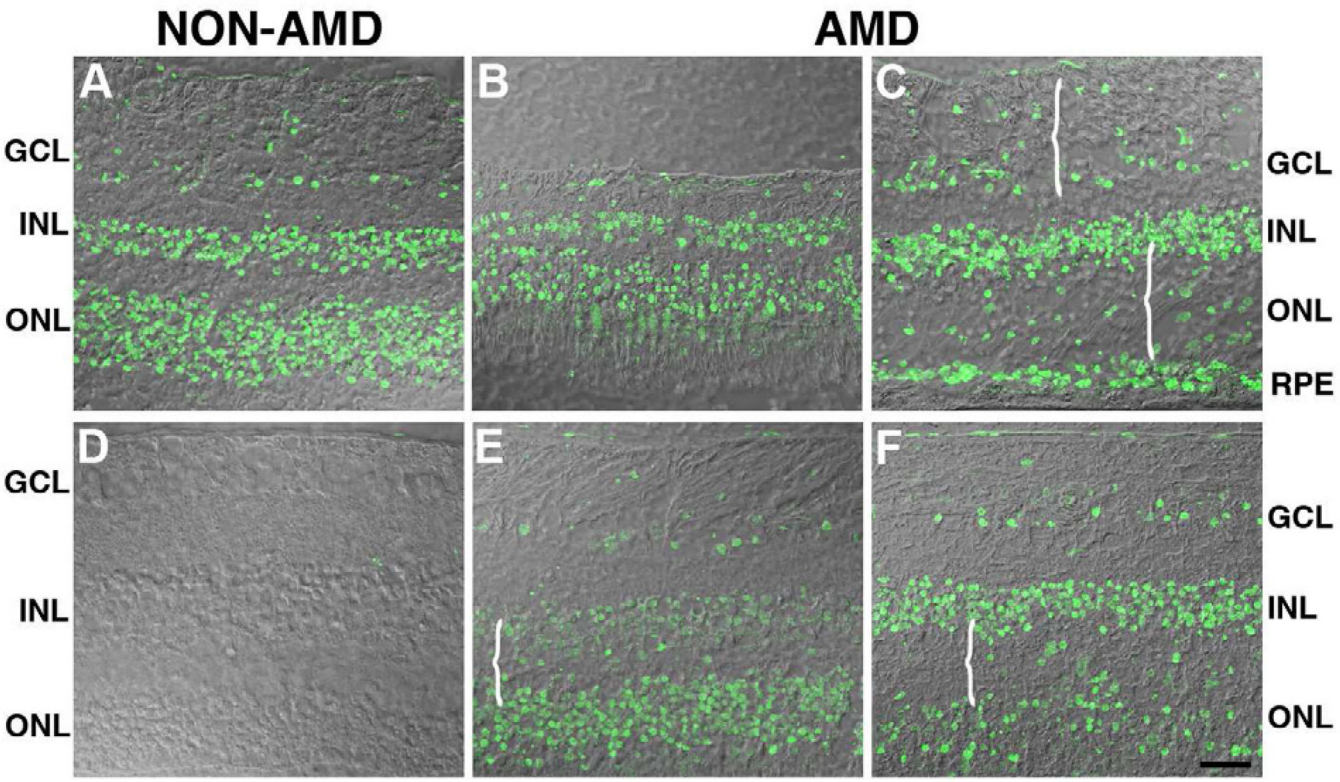

Fig. 2. Protein deimination localization is similar in the retinas of AMD and non-AMD donors

The levels of protein deimination staining were analyzed in the perimacular area of non-AMD (A) and AMD retinas (B, C, E, F). Immunoreactivity was overlaid on differential contrast images (DIC) of the retina. Analysis of the AMD retinal sections showed that the levels of deiminated proteins observed were similar to the levels observed in non-AMD retinas. Specifically, non-AMD retinas displayed protein deimination in the ganglion cell layer (GCL), inner nuclear layer (INL), outer nuclear layer (ONL). Interestingly, deimination was frequently localized to the nuclei of cells in these layers of both AMD and non-AMD. A disorganized distribution of deiminated proteins was visible in the degenerated areas of the retinas of AMD donors (braces). Non-AMD (D) and AMD (data not shown) retinas labeled only with the secondary antibody did not display any deiminated protein labeling Bar = 40μm.

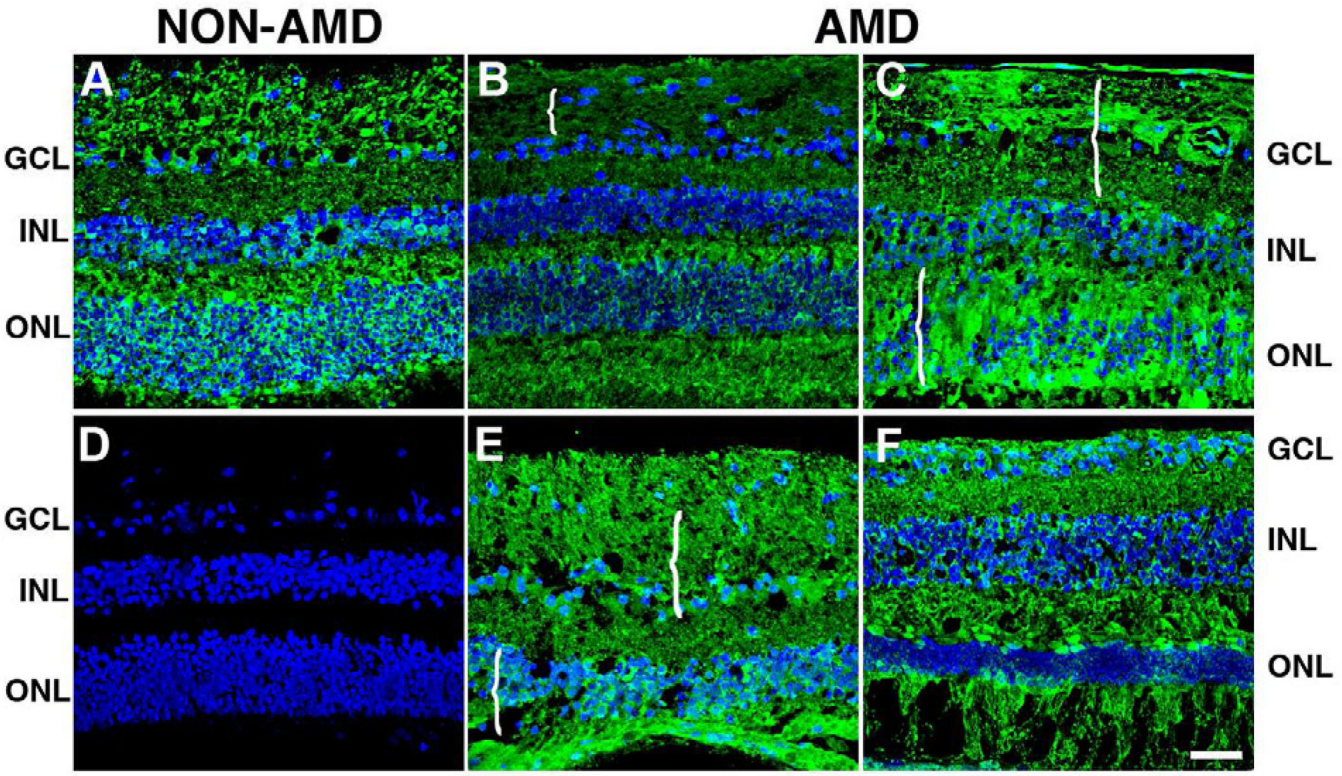

Fig. 3. PAD2 levels are similar in the retinas of AMD and non-AMD donors

The levels of PAD2 were analyzed in the perimacular area of non-AMD (A, D) and AMD retinas (B, C, E, F). Nuclei were labeled with TO-PRO3 and are shown in blue to serve as a reference for the retinal layers. Analysis of the AMD retinal sections showed that the levels of PAD2 were similar to the levels observed in non-AMD retinas. Immunolocalization of PAD2 was present in all retinal layers, namely, ganglion cell layer (GCL), inner nuclear layer (INL), outer nuclei layer (ONL). Interestingly, PAD2 was frequently localized to the nuclei of cells in the GCL and INL. A disorganized distribution of PAD2 was visible in the degenerated areas of the retinas of AMD donors (braces) Non-AMD (D) and AMD (data not shown) retinas labeled only with the secondary antibody did not display any deiminated protein labeling. Bar = 40μm.

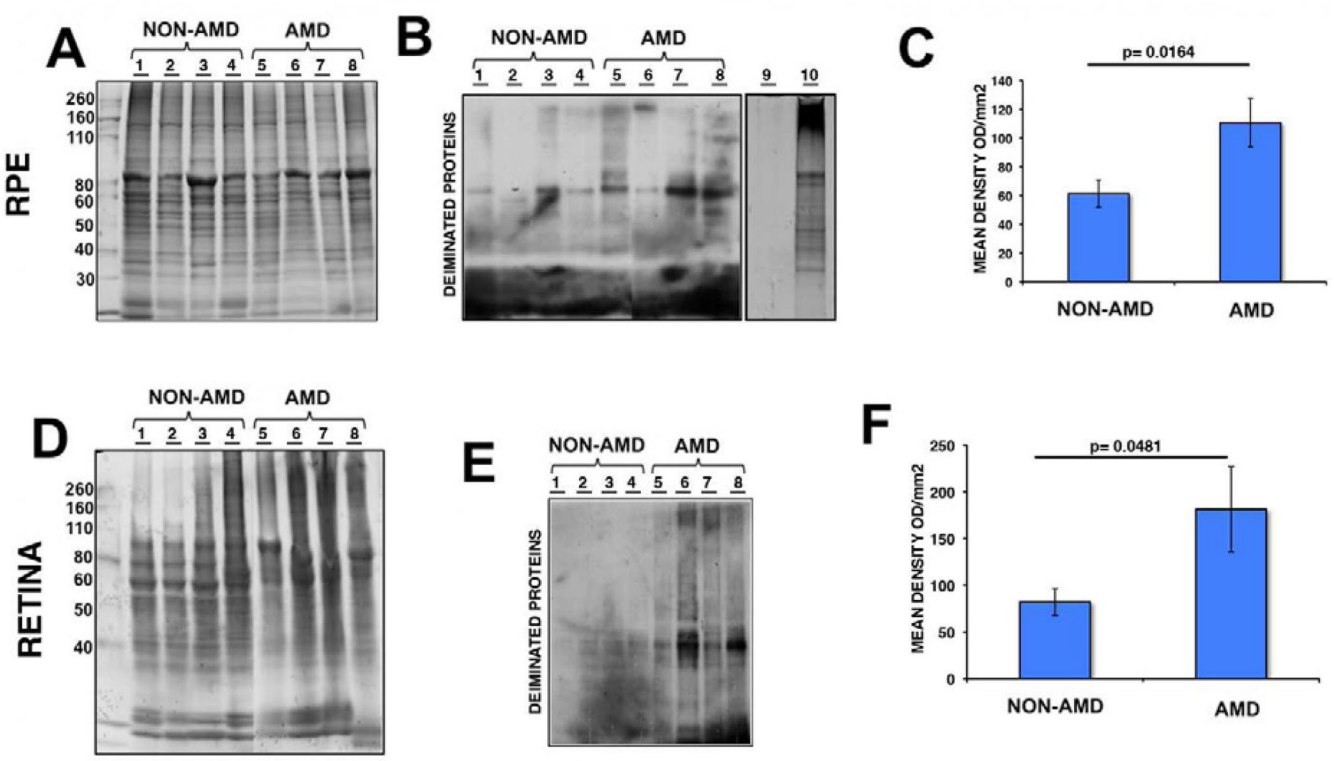

Fig. 4. Increased expression of deiminated proteins in RPE and retina lysates of AMD and non-AMD donors

RPE (A–C) and retinas (D–F) from several AMD donors were harvested and lysed. A representative gel is shown stained with Gelcode blue after partial transfer to PVDF membranes to serve as a reference for the load homogeneity of the samples (A, D). The same samples are also shown after immunoreactivity of samples with the anti-citrulline antibody (B, E). Drosophila whole extract (which lacks PADs) before (B, lane 9) and after (B, lane 10) incubation with PAD2 provided control for anti-citrulline antibody immunoreactivity. In C, and F, the mean signal intensity was plotted for AMD and non-AMD samples ± error bars. Protein deimination immunoreactivity was approximately 1.8 fold higher in AMD RPE compared with non-AMD RPE ($p = 0.0164$ by Student's t-test, $n= 10$). In addition, protein deimination immunoreactivity was approximately 2.2 fold higher in AMD retinas compared with non-AMD retinas ($p = 0.0481$ by Student's t-test, $n= 7$).

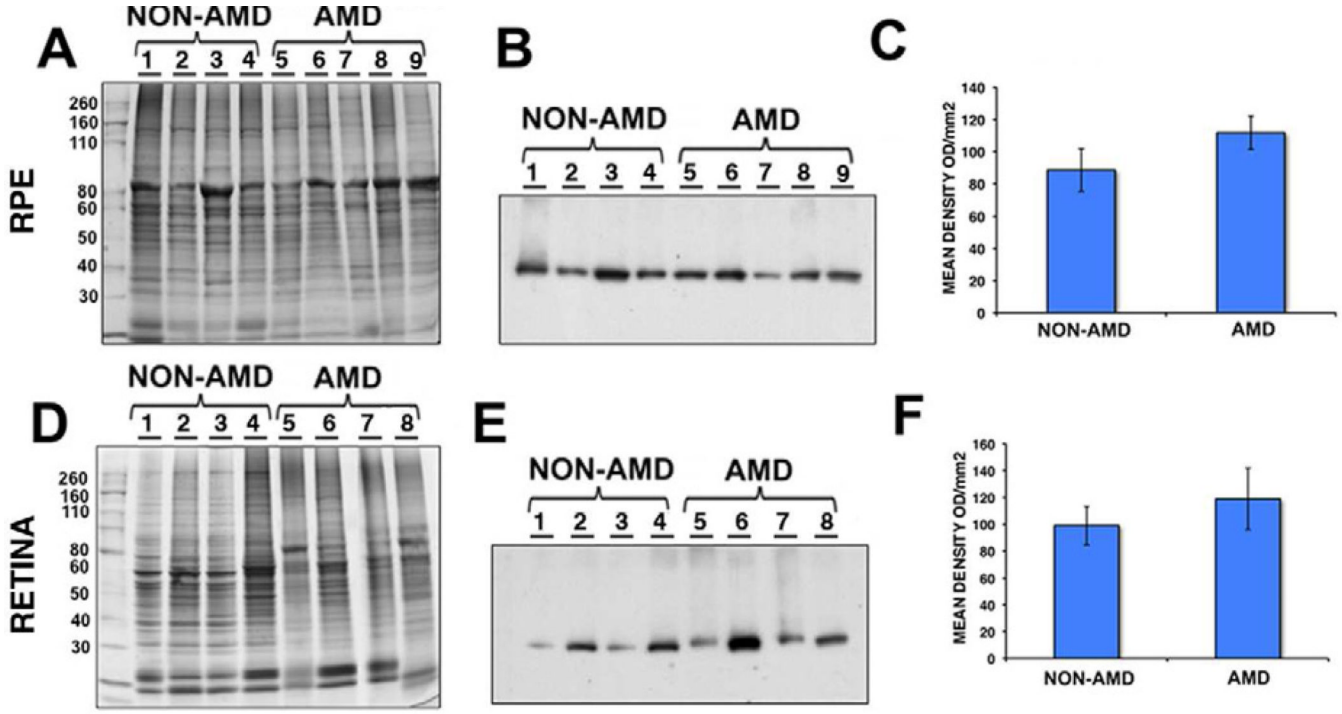

Fig. 5. Similar expression of PAD2 in RPE and retina lysates of AMD and non-AMD donors

RPE (A–C) and retinas (D–F) from AMD donors were harvested and lysed. A representative gel is shown stained with Gelcode blue after partial transfer to PVDF membranes to serve as a reference for the load homogeneity of the samples (A, D). The same samples are also shown after immunoreactivity of samples with the anti-PAD2 antibody (B, E). In C, and F, the mean signal intensity was plotted for AMD and non-AMD samples ± error bars. PAD2 immunoreactivity was approximately 1.2 fold higher in AMD RPE compared with non-AMD RPE ($p = 0.2193$ by Student's t-test, $n= 10$). PAD2 immunoreactivity was also approximately 1.2 fold higher in AMD retinas compared with non-AMD retinas ($p = 0.4535$ by Student's t-test, $n= 9$).

Exp Eye Res. Author manuscript; available in PMC 2014 June 01.

Table 1

AMD and non-AMD Human Donor Additional Information.

Donor ID	Age[a]	Gender[b]	Race[c]	PMI[d]	Donor Type
1	84	M	C	10	AMD
2	92	F	C	10	AMD
3	75	M	C	10	AMD
4	83	M	C	10	NON-AMD
5	91	F	C	10	NON-AMD
6	73	M	C	10	NON-AMD
7	63	M	C	8	NON-AMD
8	74	F	AA	8.5	NON-AMD
9	79	F	C	11	AMD
10	83	M	C	7.5	AMD
11	87	F	C	4	AMD
12	93	M	C	4.5	AMD
13	97	M	C	6	AMD
14	70	F	C	6	AMD
15	80	M	C	<6	NON-AMD
16	80	M	C	5	AMD
17	80	M	C	4.5	NON-AMD
18	80	M	C	2.5	NON-AMD
19	82	M	C	12	AMD
20	81	M	C	8	NON-AMD
21	91	M	C	<6	NON-AMD
22	35	M	C	7	NON-AMD
23	72	M	C	12	AMD
24	80	M	C	2	AMD
25	82	F	C	9	NON-AMD
26	81	F	C	4.5	NON-AMD
27	72	F	C	5.1	NON-AMD
28	50	F	C	8.5	NON-AMD

Donor ID	Age[a]	Gender[b]	Race[c]	PMI[d]	Donor Type
FFB#703	23	M	C	19	AMD
FFB#704	93	U	U	8.5	AMD
FFB#711	83	U	U	13	AMD
FFB#714	82	F	C	6.5	AMD
FFB#716	80	F	C	35.5	NON-AMD
FFB#722	90	M	C	22	AMD
FFB#723	76	M	C	9.5	AMD
FFB#728	91	M	C	7.5	AMD
FFB#745	65	F	C	7.5	NON-AMD
FFB#758	91	F	C	7	AMD
FFB#781	80	F	C	9	AMD

[a]Age: Age at death (years);

[b]Gender: M = Male, F= Female, U = Unknown;

[c]Race: C = Caucasian, AA= African american, U = Unknown;

[d]Interval from death to preservation (hrs).

Table 2

Minor Allele Frequencies (MAF) for the SNPs Genotyped in AMD and non-AMD Donor Eyes.

SNP	Risk Allele	MAF AMD	MAF Non-AMD	p-value
rs1061170 (*CFH*)	C	0.40	0.36	1.000
rs10490924 (*ARMS2*)	T	0.28	0.23	0.772
rs11200638 (*HTRA1*)	A	0.28	0.23	0.772
rs2230199 (*C3*)	G	0.19	0.15	1.000